ARCHIVES OF ELECTRICAL ENGINEERING VOL. 67(4), pp. 913–923 (2018)

DOI 10.24425/aee.2018.124749

Identification of temperature and hardness distribution during dual frequency induction hardening of gear wheels

JERZY BARGLIK

Silesian University of Technology
Krasińskiego 8, Katowice, Poland
e-mail: jerzy.barglik@polsl.pl

(Received: 20.07.2018, revised: 01.10.2018)

Abstract: Induction surface hardening means the hardening of a thin zone of the material only, while its core remains soft. The paper deals with the modelling of the Consecutive Dual Frequency Induction Hardening (CDFIH) of gear wheels and its validation. For gear wheels with modulus m smaller than 6 mm a contour profile of hardness distribution could be obtained. The investigated gear wheel is heated first by a medium frequency inductor to the temperature approximately equal to the modified lower temperature $Ac_{1\mathrm{m}}$. It means beginning of the austenite transformation. Then the gear wheel is heated by the high frequency inductor to the hardening temperature making it possible to complete the austenite transformation and immediately cooled. In order to design the process it is necessary to identify modified critical temperatures and to obtain expected temperature distribution within the whole tooth.

Key words: critical temperatures, coupled problem, electromagnetic field, temperature field, induction contour hardening

1. Introduction

The induction surface hardening (ISH) process means the hardening by induction of a thin outer zone of the material only and keeping soft its internal part [1, 2]. The result of such an induction heat treatment is a requested value of hardness in a thin outer (surface) zone with a changed, typically martensitic microstructure. The quantity of hardness and kind of obtained microstructure depend on many factors including a type of steel (its hardenability) and cooling rate. The internal part of the treated body is characterized by lower hardness (often exactly the same as before the process) and the prior microstructure. As a result of the ISH process we often notice the transition, a partially hardened zone located between the fully hardened surface zone and unchanged internal part. The transition zone has lower hardness and a mixed microstructure

containing partly martensite, but also some additions of bainite, unsolved ferrite, pearlite and residual austenite.

The role of the ISH processes and their practical application in industry still increases. There are several reasons for such development like: big efficiency connected with a heat source located close to the hardened part of the body, possibility to regulate the thickness of the hardened zone. It is a very effective method of surface hardening in comparison with classic surface hardening methods like, for instance, carbonizing [1]. In order to obtain a very thin hardened depth zone the high single frequency induction hardening system is applied. It is especially often applied for steel elements with simple regular shapes like for axi-symmetrical or flat bodies. Recently such kind of the ISH processes are used also for elements of complex shapes like gear wheels [3]. An exemplary hardness profile for a tooth of a gear wheel is presented in Fig. 1. Zone 1 represents a thin contour zone which is fully hardened with a hardness of 620, . . . , 720 HV and has the martensitic microstructure. Zone 2 is a partially hardened transition zone characterized by lower hardness and mixed microstructure. Zone 3 is not hardened with the hardness lower than 450 HV and partially changed microstructure only. And finally zone 4 means the core of the material with the prior, unchanged microstructure. For such a kind of hardening and because of the non-uniform temperature distribution within the tooth after induction heating we could achieve four zones of different metallurgical properties: hardness and microstructure.

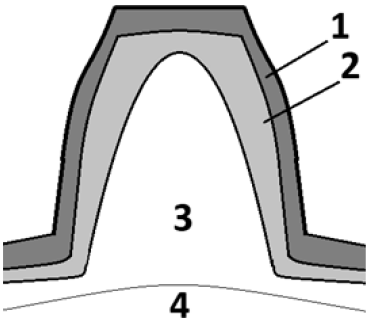

Fig. 1. Tooth of the gear wheel in the cross section with depicted profile of hardness distribution: 1 – fully hardened contour zone; 2 – partially hardened transition zone; 3 – not hardened internal part; 4 – core (prior material)

The paper concentrates on the identification of the time evolution of temperature and its spatial distribution during numerical simulation of the CDFIH process. Based upon that the hardness distribution is determined. Computations are verified by experiments. The task is rather complicated because of the high speed of induction heating and difficulties connected with the influence of an electromagnetic field on measurement equipment.

2. Kinds of ISH processes

The ISH processes are divided into two main sub-groups [4]:

– Continual induction surface hardening (CISH),

– Spin induction surface hardening (SISH).

In general, long and/or large elements require the CISH methods also known as the scan hardening. Smaller elements are hardened mostly by the SISH methods.

The CISH methods could be realized as a vertical, horizontal or circumferential kind of treatment. As an example of the vertical CISH method the induction hardening of long prismatic bodies like files of different shapes could be considered. It is described in [5]. As a case study of the horizontal CISH method the induction hardening of conical mandrels used as a tool for tube manufacturing [6] or long tubes applied in underground mining for sand transportation [7] has been presented. As an example of the circumferential CISH method the induction hardening of circular saws applied for cutting of slabs in continuous casting lines of steel is described in [8]. Such a method is also known as the part-by-part induction hardening (PPIH). Another continual method is the tooth-by-tooth induction hardening (TTIH) described for instance in [9].

The SISH means the completely hardened zone is first heated and then cooled. It is realized in a different configuration, arrangement and supply systems:

- single frequency induction hardening (SFIH),
- simultaneous dual frequency induction hardening (SDFIH),
- consecutive dual frequency induction hardening (CDFIH).

The SFIH process is realized for small workpieces, especially for these with regular shapes. In the case of gear wheels the usage of the SFIH treatment causes a completely non-uniform hardness pattern. For the medium frequency SFIH process, at which a typical range of the MF frequency is about 5, . . . , 50 kHz, it is very difficult to heat up uniformly both the tip and root of the tooth. We could obtain the profile as in Fig. 2(a), where only the root is hardened or, with a longer heating time (the profile in Fig. 2(b)), where the entire tooth is hardened.

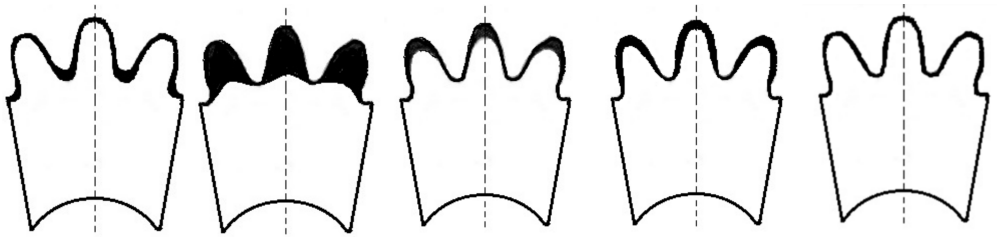

Fig. 2. Different hardening profiles [1]: (a) root hardening; (b) entire tooth hardening; (c) tip hardening; (d) non-uniform contour hardening; (e) uniform contour hardening

For the high frequency SFIH process (a typical frequency for such a treatment is bigger than 100 kHz) practically only the tip of the tooth is hardened (Fig. 2(c)). This example of application of the SFIH process for gear wheels is described, for instance, in [10]. In order to obtain the contour hardening profile shown in Figs. 2(d), (e) the SDFIH or CDFIH processes should be applied. For the SDFIH process it is more easily to obtain the uniform hardening profile. Details are described, for instance, in [11]. For the CDFIH, the non-uniform hardening profile is usually achieved. In order to compare the shape of the contour hardening profile for different cases a simplified coefficient k is introduced. It is defined as:

$$k = \frac{H}{h} = \frac{h - b + c}{h}, \tag{1}$$

where H denotes the height of the hardness profile at the tip, h is the height of the tooth, b is the thickness of the hardening zone at the tip, c is the thickness of the hardening zone at the root. (see Fig. 3).

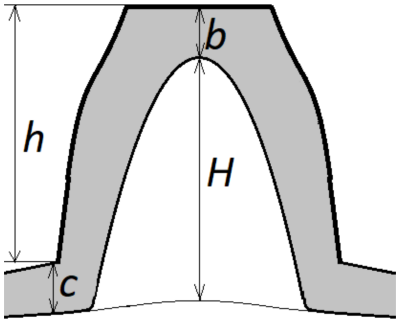

Fig. 3. Definition of the k coefficient

Determination of b and c is based upon the standard DIN EN 10328 [12] which describes the way of determination of the surface depth hardening (SDH) coefficient. If the shape of the contour zone is uniform the dimensionless coefficient $k = 1$.

The SDH coefficient is defined by relation (2) illustrated in Fig. 4.

$$\text{SDH} = d\Big|_{HV=0.8HV_0} \quad \text{for} \quad HV_{\min} \le HV_0 \le HV_{\max}, \tag{2}$$

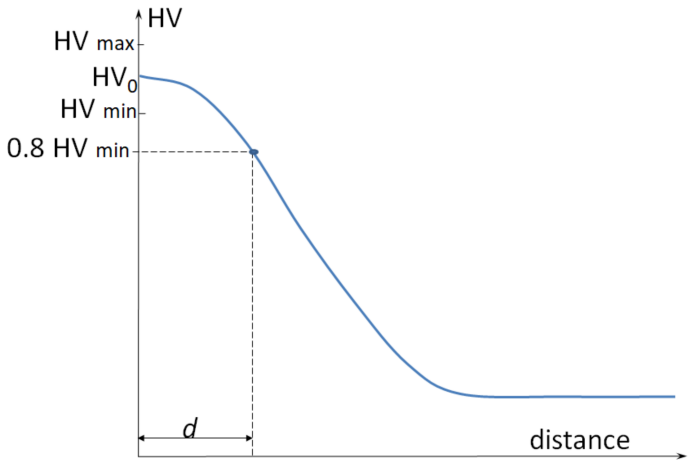

Fig. 4. Definition of the surface hardness depth (SHD) coefficient

It is the distance between the surface and the location in the layer, where the hardness in Vickers degrees equals the limit of 0.8 times its value of the surface hardness.

The CDFIH process consists of three consecutive stages: dual frequency induction heating, extremely short austenitization and intensive cooling. Let us consider exemplary temperature dependence on time in the surface zone of the body for the CDFIH process (Fig. 5).

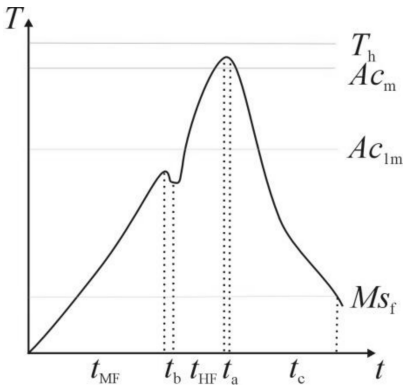

Fig. 5. Exemplary temperature dependence on time in the surface zone of the body for the CDFIH process (notations in the text) [13]

The investigated gear wheel is heated first during time t_{MF} by the medium frequency (MF) inductor to the temperature guaranteeing the beginning of the austenite transformation:

$$T\Big|_{t=t_{MF}} < Ac_{1m}(v_{ih}), \tag{3}$$

where Ac_{1m} denotes the modified lower critical temperature and v_{ih} is the average velocity of induction heating.

After a short time break (t_b) it is possible to switch off the MF inductor and remove the gear wheel to the next position. Then the gear wheel is heated by the high frequency (HF) inductor to the temperature guaranteeing the completion of the homogenous austenite microstructure.

$$T\Big|_{t=t_{MF}+t_b+t_{HF}+t_a} > Ac_m(v_{ih}), \tag{4}$$

where Ac_m denotes the modified critical temperature, t_a is the austenitization time.

The austenitization time t_a means a break between induction heating and cooling. It is very small (tens of milliseconds). If we had a smaller final temperature after induction heating and the austenitization, the austenite microstructure could not have been fully uniform.

$$Ac_m(v_{ih}) \geq T|_{t=t_{MF}+t_b+t_{HF}+t_a} \geq Ac_{3m}(v_{ih}), \tag{5}$$

where Ac_{3m} denotes the modified upper critical temperature (not depicted in Fig. 5).

The hardening temperature T_h could have been slightly bigger than the modified critical temperature Ac_m.

$$T_h = T\Big|_{t=t_{MF}+t_b+t_{HF}+t_a} + \Delta T, \tag{6}$$

where $\Delta T = 20, \ldots, 40°C$.

The process is terminated by cooling which is realized by spraying or by merging the body into a container with quenchant. Let us consider the most commonly applied method of cooling by spraying. The obtained hardness and microstructure distributions depend mainly on a kind of quenchant and on the cooling rate. There are two critical temperatures related to the cooling process: the Martensite Start Temperature *Ms* guaranteeing the beginning of the martensite transformation (not depicted in Fig. 5) and the Martensite Finish Temperature Ms_f guaranteeing

its termination. As a final result, after intensive cooling with the velocity v_c being bigger than its critical value $v_{c\,min}$ to the temperature smaller than the Martensite Finish Temperature Ms_f

$$v_c > v_{c\,min} \; T\Big|_{t=t_{MF}+t_b+t_{HF}+t_a+t_c} \leq Ms_f(v_c), \tag{7}$$

we obtain thin surface zone with fully hardened material having martensitic microstructure.

Dependence of all three critical temperatures on velocity of induction heating v_{ih} will be discussed in the next chapter.

Modelling of the process requires the analysis of coupled electromagnetic and thermal fields during induction heating and thermal and hardness fields during cooling [3].

3. Determination of critical temperatures

In order to design properly the CDFIH technology it is necessary to determine by measurements the modified critical temperatures for heating (Ac_m, Ac_{3m}, Ac_{1m}) and for cooling (Ms, Ms_f). The determination is described based upon an example of the CDFIH process provided for small gear wheels made of steel AISI 4340. The alloy additions of the investigated steel is collected in Table 1.

Table 1. Chemical composition of steel AISI 4340 (alloy additions) [15]

Element	C	Si	Mn	Cr	Ni	Mo	V	Cu
% mass	0.41	1.63	0.83	0.83	1.91	0.41	0.08	0.03

Modified critical temperatures for induction heating are determined based upon the time-temperature-austenitization (TTA) diagram (Fig. 6) for investigated steel [16].

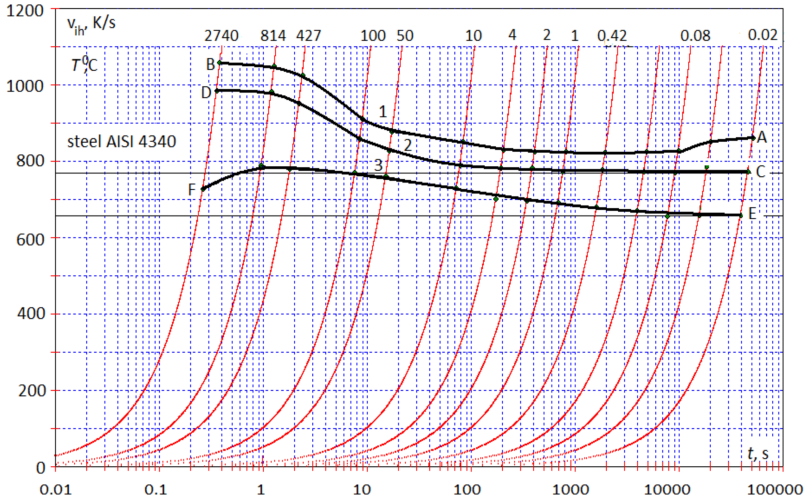

Fig. 6. TTA diagram for steel AISI 4340: 1 – $Ac_m(v_{ih})$; 2 – $Ac_{3m}(v_{ih})$; 3 –$Ac_{1m}(v_{ih})$

Curve 1 at Fig. 6 represents the dependence of Ac_{m} on velocity of induction heating v_{ih}. For slow, conventional heating (v_{ih} = 0.02 K/s) Ac_{m} = 861°C (point A at the curve 1). For fast heating the modified critical temperature Ac_{m} is distinctly bigger. For a very high velocity of heating v_{ih} = 2 740 K/s Ac_{m} = 1 065°C (point B at the curve 1). Curves 2 and 3 represent the dependences of the modified upper critical temperature $Ac_{3\mathrm{m}}$ representing completion of the austenite transformation and the modified lower critical temperature $Ac_{1\mathrm{m}}$ representing the beginning of the austenite transformation on velocity of induction heating v_{ih}, respectively. For the rapid heating $Ac_{3\mathrm{m}}$ = 990°C (point D at the curve 2) and $Ac_{1\mathrm{m}}$ = 770°C (point F at the curve 3).

In order to determine the hardness and the microstructure distributions within the whole zones of the tooth several continuous-cooling-temperature (CCT) diagrams measured from the hardening temperature T_{h} = 960, . . . , 1 050°C have been considered. The exemplary diagram for T_{h} = 1 050°C is shown in Fig. 7.

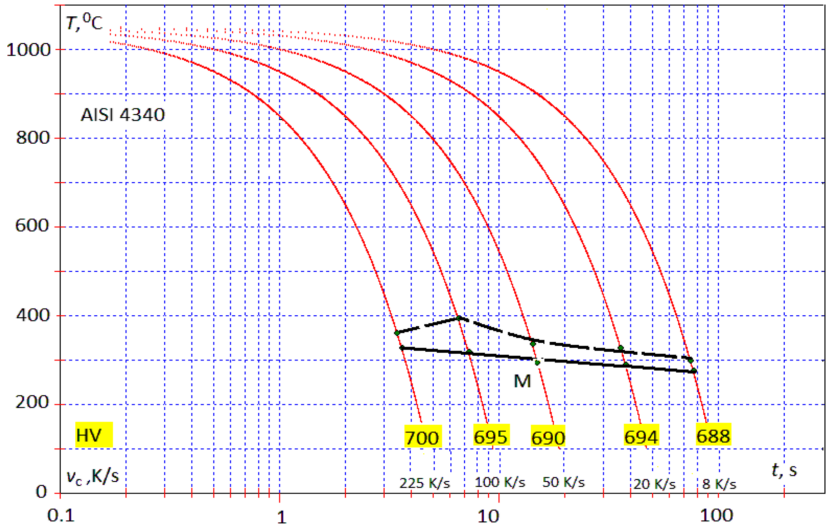

Fig. 7. CTT diagram for steel AISI 4340 (AMS 6414)

Dependences of Martensite Start Temperature *Ms* (line —) and martensite finish temperature Ms_{f} (line - -) on velocity of cooling v_{c} for the hardening temperature T_{h} = 1 050°C are depicted in Fig. 7. Based upon the presented CTT diagram for slow cooling with the velocity v_{c} = 8 K/s critical temperatures are equal to: *Ms* = 282°C and Ms_{f} = 307°C. For more intensive cooling (v_{c} = 100 K/s) the critical temperatures are equal to: *Ms* = 306°C and Ms_{f} = 390°C. If the cooling rate v_{c} is in the range of 8, . . . , 225 K/s the martensitic microstructure is noticed and the hardness is in the range of 688, . . . , 700 HV. Of course at the beginning of cooling and during the process the temperature is a function of spatial coordinates, so in order to determine hardness and microstructure distributions in the whole tooth, it is necessary to take into consideration corresponding values of velocity of cooling and critical temperatures *Ms*, Ms_{f} for cooling.

4. Example of the CDFIH system

Let us consider the CDFIH system from Fig. 8. At the beginning, the gear wheel 3 made of the investigated steel AISI 4340 mounted at the rotating mandrel, 5 is located inside of the MF inductor 1 and heated to the temperature of about the lower critical temperature Ac_{1m}. Then it is quickly removed to the next position inside the HF inductor 2, equipped with a flux concentrator. When the temperature reaches the assumed hardening temperature T_h, the gear is removed to the final position inside the sprayer 4. The mixture of water and polymer solution is applied as a quenchant. In order to improve the electrical efficiency of the MF and HF heating, the inductor-gear wheel systems lengths of MF bus-bars 6 and HF bus-bars 7 and corresponding distances between their profiles are set as low as possible.

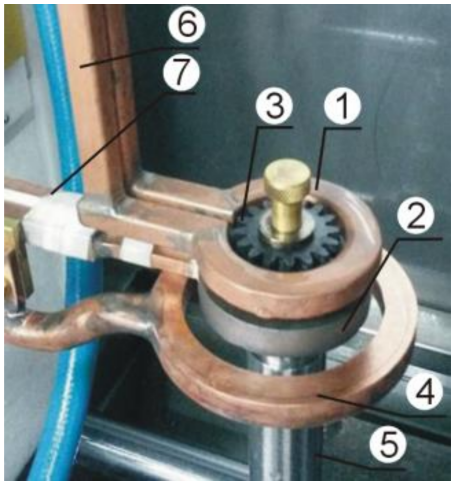

Fig. 8. CDFIH system: 1 – MF inductor; 2 – HF inductor with flux concentrator; 3 – gear wheel; 4 – sprayer; 5 – mandrel; 6 – MF bus-bars, 7 – HF bus-bars

The basic dimensions and parameters of the inductor-sprayer system are as follows:

The gear wheel: the teeth number $n = 16$, the width of the tooth ring $b = 0.006$ m, the external diameter $d_e = 0.0356$ m, the internal diameter $d_i = 0.0269$ m, the diameter of the hole $d_h = 0.016$ m,

The MF inductor: the number of turns $n = 1$, height $h_{MF} = 0.007$ m, external diameter $d_e = 0.054$ m, internal diameter $d_i = 0.0395$ m,

The HF inductor: the number of coils $N = 1$, the height of the coil $H_{HF} = 0.007$ m, the total height including the magnetic flux concentrator $H_t = 0.021$ m, the external diameter $D_e = 0.061$ m, the internal diameter $D_i = 0.0395$ mm,

The sprayer: the internal diameter $d_{si} = 0.064$ m, the external diameter $d_{se} = 0.090$ m, the height $h_{se} = 0.009$ m, the quenchant – Aqua Quench 140.

Computations have been realized by means of the 3D Flux software for calculation of the coupled electromagnetic and temperature field during induction heating and cooling as well as QT steel software, supported by several personally developed procedures for calculation of hardness and microstructure fields [16]. The influence of dependences of material properties on temperature and magnetic field intensity was described, for instance, in [10, 17, 18]. The time dependence of temperature for the whole tooth during the process (induction heating, very short

austenitization (hundreds milliseconds or less) and cooling) has been calculated and recorded. The temperature distribution within the cross-section of the tooth for the time of the induction heating t_{ih} = 3.5 s is presented in Fig. 9.

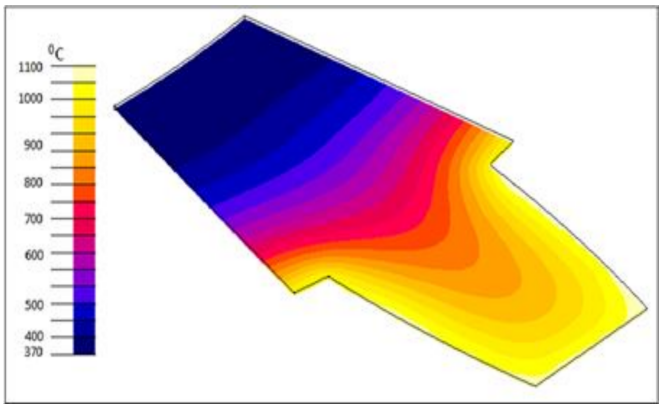

Fig. 9. Calculated temperature distribution within the cross-section of the tooth after induction heating

For $t = t_{ih}$ the average temperature in the surface zone with the thickness g = 0.0015 m equals T_{av} = 1 023.5°C. The average velocity of induction heating in the same zone equals v_{ih} = 325 K/s, which means the following values of the modified critical temperatures at the working surface along the line A, . . . , G (see Fig. 10): Ac_m = 1 000.5°C, Ac_{3m} = 948.5°C, Ac_{1m} = 796°C. So, the average temperature in the hardened zone is sufficiently higher than the modified upper critical temperature Ac_{3m}. The temperature distribution along the line A, . . . , G at the working surface of the tooth (point A is located at the root of the tooth and point G at the tip of the tooth) is presented in Fig. 10.

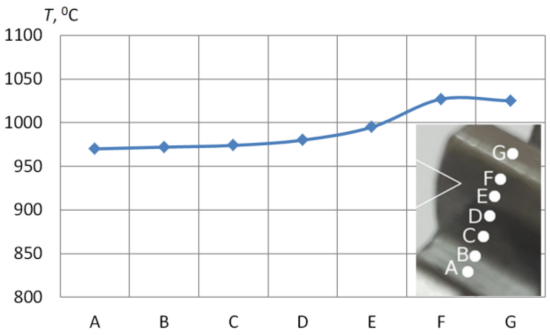

Fig. 10. Calculated temperature distribution along line A–G

During experiments at the laboratory stand located at the Silesian University of Technology, the temperature is measured by means of specialized measuring and registration systems containing the specialized pyrometer, cameras and computer registration [19]. They make it possible to determine: the temperature in the selected point (in the analyzed case in point G) and the average temperature within the top plane of the gear wheel. However accuracy of such measurements are

rather limited. So, in order to verify the computations, it is necessary to compare computed and measured hardness distribution. The result of such a comparison is presented in Fig. 11.

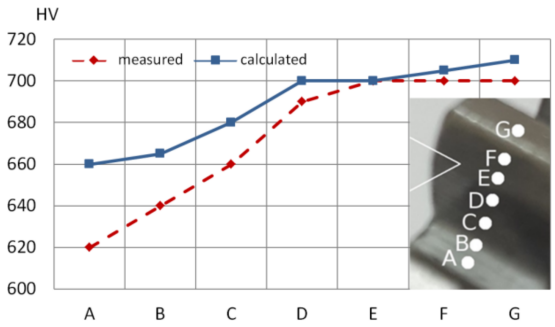

Fig. 11. Comparison of calculated and measured hardness in Vickers degrees

For hardness distribution, the QT steel software with some single, personally developed numerical procedures, is applied. Measurements of hardness is realized by means of microhardness meter Vickers FM700 [20]. For the purpose of comparison, the gear wheel is not tempered. The non-uniform shape of the contour zone is obtained. The SDH coefficient changes from 0.001 m at point A located at the root till 0.002 m at point G on the tip. The dimensionless coefficient of the contour zone equals $k = 0.8$. Reasonable, practically accepted accordance between computations and measurements is achieved.

5. Conclusions

The accuracy of numerical modeling of the CDFIH process depends on many factors including correct selection of such parameters like: hardening temperature, heating and cooling rates, material properties and their dependence on temperature, heat transfer parameters etc. In order to select correct values of the hardening temperature, the dependence of critical temperatures on velocity of induction heating should be taken into consideration. Such dependences should be determined from the TTA diagram by measurements provided for samples of investigated steel. Hardness distribution should be determined by means of several CCT diagrams started from different hardening temperatures. Reasonable (less than 7.5%) accordance between computations and measurements is achieved. A reason of such inaccuracy is connected with simplification of the computation model (uncertainty of some input data like material properties and their dependence on temperature, limited accuracy of modified critical temperatures for heating and cooling etc.). Next steps of the research should be aimed at the improvement of applied temperature measurement systems.

Acknowledgements

The paper was prepared within the project PBS2/A5/41/2014 of the National Center for Research and Development.

References

[1] Rudnev V., Totten G., *Induction Heating and Heat Treatment*, ASM International (2014).

[2] Barglik J., Ducki K., *Mathematical Modelling of continual induction surface hardening of axi-symmetric bodies*, Archives of Electrical Engineering, vol. 54, no. 4, pp. 479–487 (2005).

[3] Barglik J., *Induction hardening of steel elements with complex shapes*, Przegląd Elektrotechniczny, vol. 94, no. 4, pp. 51–54 (2018).

[4] Barglik J., *Induction surface hardening – comparison of different methods*, Przegląd Elektrotechniczny, vol. 94, no. 7, pp. 6–11 (2018).

[5] Doležel I., Barglik J., Sajdak C., Škopek M., Ulrych B., *Modelling of Induction Heating and Consequent Hardening of Long Prismatic Bodies*, COMPEL – the International Journal for Computation and Mathematics in Electrical and Electronic engineering, vol. 22, no. 1, pp. 79–87 (2003).

[6] Doležel I., Barglik J., Ulrych B., *Continual induction hardening of axi-symmetric bodies*, Elselvier, Journal of Materials Processing Technology, vol. 161, no. 1–2, pp. 269–275 (2005).

[7] Barglik J., *Induction Hardening of Steel Tubes by Means of Internal Inductor*, Journal of Iron and Steel Research International, vol. 19, no. 1–2, pp. 722–725 (2012).

[8] Barglik J., Doležel I., Ducki K., Ulrych B., *Mathematical and Computer Modelling of Induction Heating and Consequent Hardening of Circular Saw*, IOS Press Studies in Electromagnetics and Mechanics, vol. 22, pp. 351–356 (2002).

[9] Midea J., Lynch D., *Induction Hardening of Gears*, Thermal Processing, no. 4, pp. 46–51 (2014).

[10] Barglik J., Smagór A., Smalcerz A., *Computer Simulation of Single Frequency Induction Surface Hardening of Gear Wheels: Analysis of Selected Problems*, International Journal of Microstructure and Materials Properties, vol. 13, pp. 4–15 (2018).

[11] Spezzapria M., Forzan M., Dughiero F., *Numerical Simulation of Solid–Solid Phase Transformations During Induction Hardening*, IEEE Transactions of Magnetics, vol. 52, no. 3, pp. 740–743 (2016).

[12] Standard DIN EN 10328, *Determination of the conventional depth of hardening after surface heating* (2005).

[13] Barglik J., Smagór A., Smalcerz A., *Induction hardening of gear wheels of steel 41Cr4*, International Journal of Applied Electromagnetics and Mechanics, vol. 57, suppl. 1, pp. S3–S12 (2018).

[14] Lupi S., *Fundamentals of Electroheat: Electrical Technologies for Process Heating*, Springer (2016).

[15] https://www.astmsteel.com/product/4340-steel-aisi, accessed April 2018.

[16] Barglik J., *Mathematical modelling of induction surface hardening*, Compel – the International Journal for Computation and Mathematics in Electrical and Electronic Engineering, vol. 35, no. 35, pp. 1403–1417 (2016).

[17] Nacke B., Wrona E., *Design of complex induction hardening problems by means of numerical simulation*, Archives of Electrical Engineering, vol. 54, no. 4, pp. 461–466 (2005).

[18] Barglik J., Smalcerz A., *Influence of the magnetic permeability on modelling of induction surface hardening*, COMPEL – the International Journal for Computation and Mathematics in Electrical and Electronic Engineering, vol. 36, iss. 2, pp. 555–564 (2017).

[19] Barglik J., Smagór A., Smalcerz A., Kopeć G., *Experimental stand for investigation of induction hardening of steel elements*, Metalurgija, vol. 57, no. 4, pp. 341–344 (2018).

[20] Wróbel T., *The influence of inoculation type on structure of pure aluminium*, Proceedings of 21st International Conference on Metallurgy and Materials, Kraków, Poland, pp. 1114–1120 (2012).